Atomistic Molecular Simulations Suggest a Kinetic Model for Membrane Translocation by Arginine-Rich Peptides

Sun, Delin; Forsman, Jan; Woodward, Clifford E.

Published in:
The Journal of Physical Chemistry Part B

DOI:
10.1021/acs.jpcb.5b08072

2015

Atomistic Molecular Simulations Suggest a Kinetic Model for Membrane Translocation by Arginine-Rich Peptides

Delin Sun,[†] *Jan Forsman*,[‡] *and Clifford E. Woodward*[*, †]

[†]School of Physical, Environmental and Mathematical Sciences, University of New South Wales, Canberra ACT 2600, Australia

[‡]Theoretical Chemistry, Chemical Centre, Lund University, P.O. Box 124, S-221 00 Lund, Sweden

ABSTRACT

Arginine-rich cell penetrating peptides (ARCPPs) are known to quickly permeate cell membranes through a non-endocytotic pathway. Potential clinical applications of this facility have prompted enormous effort, both experimental and theoretical, to better understand how ARCPPs manage to overcome the prodigious thermodynamic cost of lipid bilayer permeation by these highly charged peptides. In this work we report the results of all-atom simulations, which suggest that a kinetic (rather than thermodynamic) mechanism may explain how ARCPPs are able to achieve this. Our simulations reveal that octaarginine significantly hinders the closing of membrane pores, either individually or via aggregation in the membrane pore, while octalysine (not an ARCPP) lacks this ability. Our proposed mechanism is an alternative to current attempts to explain pore-mediated translocation of ARCPPs. It asserts that ARCPPs need not lower the equilibrium thermodynamic cost of pore formation. Instead, they can achieve rapid bilayer translocation by instead slowing down the kinetics of naturally occurring thermal pores.

1. INTRODUCTION

Numerous experimental studies have established that the cellular uptake of arginine-rich cell penetrating peptides (ARCPPs) involves a non-endocytotic mechanism,[1, 2] often linked to the unique hydrogen bonding between lipid phosphates and the guanidinium moiety.[3, 4] Nevertheless, the way in which this strong coupling facilitates the cellular uptake of ARCPPs remains largely unclear. One model suggests that ARCPPs penetrate cell membranes by binding to anionic lipids to form an inverse micelle with reduced charge.[3, 5] This is supported by experimental studies which show that oligoarginines, but not oligolysines, have increased organic solubility in the presence of amphiphilic counterions.[5] This is consistent with the observation that oligolysines have reduced ability to permeate lipid membranes.[6] Unfortunately, direct *in vivo* observation of this mechanism is not straightforward and computer simulations of oligoarginine translocation through model membranes do not support it.[7, 8] Another commonly posited model is that ARCPPs are able to permeate cell membranes by facilitating membrane pore formation.[4, 9, 10] That is, it is believed that ARCPPs are able to significantly lower the thermodynamic cost of membrane pore formation. However, there is still no generally accepted explanation as to how this is achieved by this class of peptide and not others, such as oligolysines.

In addition to experiments, simulation methods such as molecular dynamics (MD) can provide valuable insights into the qualitative mechanisms of biological processes. Recent MD simulations by us showed that oligoarginine is able to slow down collective lipid kinetics in the pore, substantially extending pore lifetimes in a zwitterionic lipid bilayer.[7] This prompted us to speculate that the ability of ARCPPs to traverse cell membranes may rely on how they affect pore dynamics, rather than their influence on pore formation itself. In fact, it has long been known that thermal fluctuations can give rise to transient membrane pores in lipid membranes anyway,[11] and it has been speculated that thermal pores may be critical for the cellular uptake of nutrients in primitive organisms.[12] However,

the rate of spontaneous pore formation is generally too low to explain membrane translocation of ARCPPs via opportunistic transport through these types of pores. Furthermore, it is hard to see how this mechanism would discriminate between ARCPPs and other groups of peptides not in this family, but of similar size and charge density. As an alternative hypothesis, we have proposed that efficient peptide transport may occur through a limited number of thermal pores that have become "associated" with peptides. Translocation becomes enhanced, provided the pore lifetime becomes comparable to the timescale of peptide diffusion, i.e., the pore remains open while the peptide remains adsorbed to its inner surface. Increasing the lifetime of thermal pores in this way allows cooperative diffusion of peptide through them. This mechanism is a conceptual departure from current attempts to explain pore-mediated translocation of ARCPPs, as it asserts that peptides need not have to lower the thermodynamic cost of pore formation to achieve rapid transport, but only slow down the kinetics of naturally occurring thermal pores. The plausibility of this mechanism remains uncertain, however, as our original simulation studies were obtained using a single force-field model (from the GROMOS suite of force fields) and no comparisons were made with other peptides, such as oligolysine. In this work, we report the results of a broader MD study, which addresses those issues. Here we investigate the equilibrium and dynamic properties of model zwitterionic and anionic lipid membranes in the presence of octaarginine (ARG8) and octalysine (LYS8) peptides. We uncover remarkably different membrane pore kinetics induced by these two peptides, consistently predicted by two different all-atom force field models. Our findings support a compelling new kinetic model for membrane translocation by ARCPPs.

2. SIMULATION METHODS

2.1 Peptide Adsorption to the Bilayer Surface

We began our study by comparing the adsorption of ARG8 and LYS8 onto a planar bilayer, consisting of 80% 1-dioleoyl-2-oleoyl-sn-glycerol-3-phosphoethanolamine (DOPE) and 20% 1-

dioleoyl-2-oleoyl-sn-glycerol-3-phosphatidylserine (DOPS) lipids. Our model system contained 96 DOPE lipids, 24 DOPS lipids, 4 peptides, 32 chloride counterions, 24 sodium counterions and 6200 TIP3P water molecules. Simulations were carried out using a semi-isotropic isothermal–isobaric (NPT) ensemble, which allows independent fluctuation in the area of the bilayer plane and the system dimension perpendicular to the bilayer. The four peptides were initially placed close to one leaflet of the bilayer which consists of 48 DOPE lipids and 12 DOPS lipids. We performed a 200 ns MD simulation on each system. In order to investigate the qualitative consistency of our results, we used two different atomistic force field models: the all-atom CHARMM36[13] and SLIPIDS/AMBER99SB-ILDN[14, 15] force fields for lipids and peptides. In previous work, we carried out systematic comparisons of widely-used force fields for the description of ionized arginine and lysine amino acid side-chains interacting with a zwitterionic lipid bilayer.[16] We did find that generally consistent results were obtained with the above force fields with respect to the interaction free energies of the side-chains with a zwitterionic lipid bilayer. Furthermore, these calculated interactions were consistent with the Wimley-White interfacial scales.[17] This notwithstanding, peptides made up from a number of side-chains are expected to amplify differences between the force fields insofar as their ability to describe peptide-lipid bilayer interactions. Thus, comparison of results from these two force field models provides a reasonably stringent test for any proposed mechanism of activity of these peptides.

2.2 Umbrella Sampling Simulations

Steered MD[18] and umbrella sampling[19] simulations were performed to derive the potential of mean force (PMF) between the peptide (either ARG8 or LYS8) and the DOPE/DOPS bilayer. In steered MD simulations, a harmonic potential with a force constant of 1000 kJ/mol/nm^2 was applied between the centre of mass of the peptide and another point on a line through the centre of mass of the bilayer. The peptide was pulled along the z-axis (perpendicular to the bilayer plane) from the bulk

water to the bilayer centre at a rate of 0.01 nm/ps. Configurations from steered MD simulations were selected every 0.1 nm along the z-axis and used as starting points for umbrella sampling simulations. Forty five windows were generated for the umbrella sampling simulations. A biased harmonic potential with a force constant of 3000 kJ/mol/nm^2 was used to confine the peptide within the sampling window and the system was simulated for 100 ns within each window (18 microseconds in total). In this way, the unbiased probability distribution functions was obtained for each window and used to construct the PMF profiles using the weighted histogram analysis method (WHAM).[20]

2.3 Kinetics of Pore Closure

We mimicked a pore formed via thermal fluctuations by using a sufficiently large membrane tension to rupture the lipid bilayer in the absence of any peptide. The ruptured lipid bilayer was then equilibrated in an isotropic NPT ensemble, which only allows uniform expansion or contraction of the system volume (in all three dimensions). This ensemble artificially stabilizes the pore, allowing lipids to adopt equilibrium configurations in the presence of this constraint. Under these conditions a toroidal-shaped membrane pore is rapidly formed. A peptide was then placed close to the membrane pore edge and MD simulations were immediately carried out in the semi-isotropic NPT ensemble (without tension) so as to allow the pore to develop without constraints. These simulations were compared to those where a peptide was not added. We also created pores by using the umbrella sampling simulations (described in the previous section). Our ability to achieve this depends upon the force field model. In the case of the CHARMM force field, both ARG8 and LYS8 created membrane pores when the peptides were constrained at the bilayer centre. While for the SLIPIDS/AMBER99SB-ILDN combination, only ARG8 gave a pore. The ability of the CHARMM force field to create membrane pores, with either peptide, also allows us to evaluate and compare the average interaction energies between the bilayer lipids and the two different peptides, while the latter are tethered within the pore (see Table 1 below). To investigate the role of bilayer charge, we

repeated these calculations using either zwitterionic DOPE and DOPC (1, 2-dioleoyl-sn-glycero-3-phosphocholine) lipids.

2.4 Bulk Phase Simulations

The simulations of ARG8 and LYS8 in bulk solutions with methyl phosphate counterions were carried out using the CHARMM force field. The system contained 5 peptides, 40 methyl phosphate counterions and 4000 water molecules and the length of the cubic simulation box was 5.1 nm. Simulations were run for 30 ns.

2.5 Effect of Salt on ARG8 Aggregation on the Bilayer Surface

To investigate whether physiological concentration of salt can lead to ARG8 aggregation on a planar lipid bilayer surface, as was reported in the work by Vazdar *et al*,[21] we carried out simulations starting with a configuration in which three ARG8 peptides were initially placed close to each other on the bilayer surface. In addition, 0.15 M NaCl was added into the solution and 10 ns of unconstrained MD simulation were run using the CHARMM force field.

2.6 Other Simulation Parameters

All simulations were performed at a temperature of 310 K. All molecular species were independently coupled to the Nosé-Hoover thermostat[22, 23] with a coupling time constant of 0.5 ps. In the case of the semi-isotropic pressure coupling method, the lateral and perpendicular pressures were independently coupled to the Parrinello-Rahman barostat[24] with a coupling time constant of 2 ps and compressibility of 4.5×10^{-5} bar^{-1}. For isotropic pressure simulations the fluctuations in the lateral and perpendicular directions were not independent. Periodic boundary conditions were employed, with the long-range electrostatic interactions treated using the particle-mesh Ewald (PME) method.[25] All bonds lengths in peptides and lipids were constrained using the LINCS algorithm[26] and

TIP3P water molecules were constrained using the SETTLE algorithm.[27] The simulation time step was 2 fs. Simulations were performed using the GROMACS 4.5.5 package.[28]

3. RESULTS AND DISCUSSION

3.1 Adsorption of ARG8 and LYS8 onto the Lipid Bilayer Surface

Four ARG8 or LYS8 peptides were initially placed close to one leaflet of the DOPE/DOPS lipid bilayer and then the system was simulated for 200 ns. We found that all ARG8 molecules adsorbed to the same leaflet, whereas the LYS8 peptides were distributed on both sides of the bilayer by diffusing across the water gap (see Figure. 1). Hence, ARG8 appears to adsorb more strongly to the anionic lipid bilayer surface than LYS8, a result which was qualitatively similar for both all-atom force fields. Recent simulations by Vazdar *et al*. found significant aggregation of oligoarginine on the anionic 1-palmitoyl-2-oleoyl-sn-glycero-3-phosphocholine (POPC)/1-palmitoyl-2-oleoyl-sn-glycerol-3-phosphatidylserine (POPS) lipid bilayer surface.[21] Aggregation was not observed in our simulations with the ARG8 peptides remaining segregated in all cases, likely due to the repulsive interactions between their substantial charges (+8). We further tested this result by placing three ARG8 peptides in an initial "aggregated" configuration on the bilayer surface, but they separated quickly within 5 ns (see Figure. 2). Vazdar *et al*., not only used a different (Berger/OPLS-AA) force field combination, but their simulation also contained 0.125 M NaCl. Screening of the long-ranged electrostatic repulsion between peptides by the salt could enable attractive interactions between the guanidinium ions to promote aggregation. We investigated the role of salt by adding 0.15 M NaCl to our system. Three ARG8 peptides were initially placed in an "aggregated" configuration on the DOPE/DOPS bilayer surface. However, the peptide aggregate quickly dissociated within 5 ns (see Figure 2). Thus, it appears that aggregation of oligoarginine on the bilayer surface may depend either on the type of lipid or the force field employed. Neither of the all-atom force fields used in

our work predicted aggregation on the planar bilayer, however, this was not the case in the presence of pores, as will be shown below.

Our finding that ARG8 but not LYS8 peptides co-adsorb onto one leaflet of the bilayer can be ascribed to a stronger attraction between ARG8 and the lipid/water interface. The adsorption of all ARG8 molecules on a single surface is not likely the free energy minimum, but a metastable state eventuating from the opportunistic binding of peptides to the nearest leaflet. It is indicative that ARG8 molecules will distribute themselves across both leaflets in a purely zwitterionic DOPE bilayer, as shown in Figure S1. This result indicates the binding affinity of ARG8 is strongly influenced by the anionic lipid composition of the bilayer.

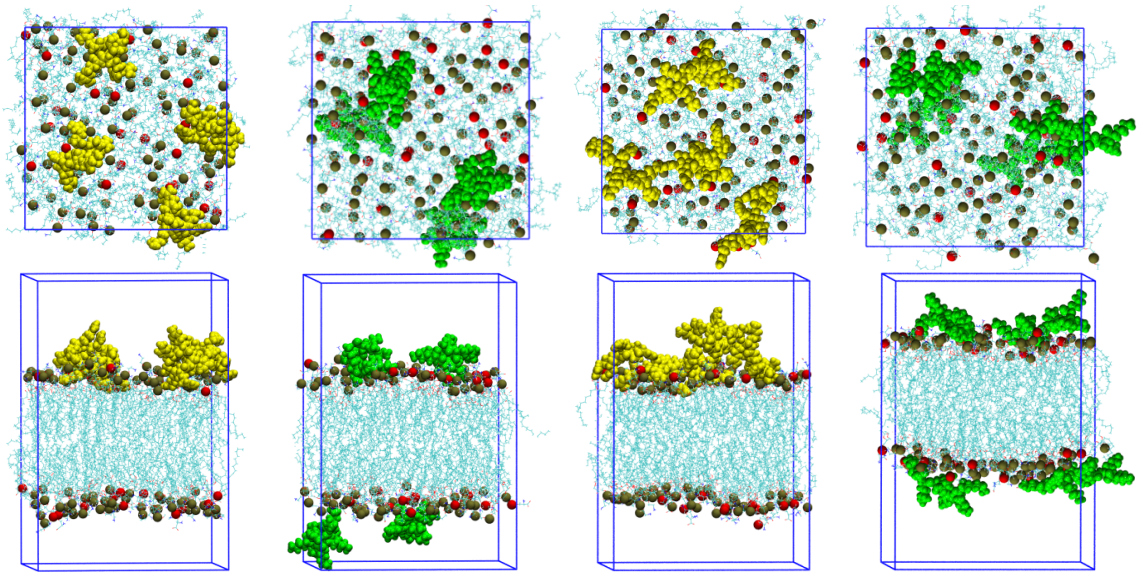

Figure 1. *Top and side views of four ARG8 and LYS8 peptides adsorbed onto the DOPE/DOPS lipid bilayer. (A) ARG8; CHARMM force field; (B) LYS8; CHARMM force field; (C) ARG8; SLIPIDS/AMBER99SB-ILDN force field; (D) LYS8; SLIPIDS/AMBER99SB-ILDN force field. The lipid bilayer contains 96 DOPE lipids and 24 DOPS lipids. The phosphorous atoms on DOPS and DOPE lipids are colored red and tan respectively. Water molecules are not shown for clarity.*

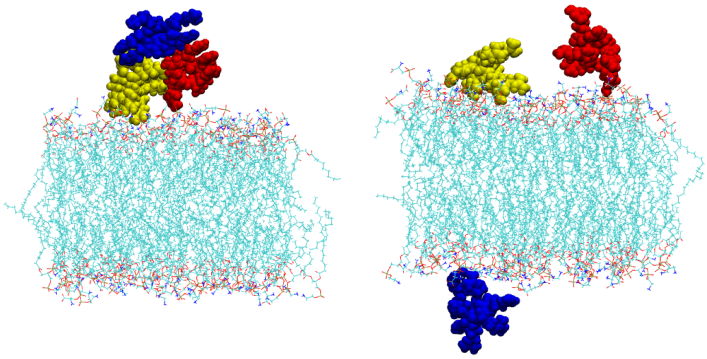

0 ns 5 ns

Figure 2. *These snapshots show that ARG8 cannot aggregate on the surface of DOPE/DOPS lipid bilayer even in the presence of 0.15 M salt. The three ARG8 peptides were initially aggregated, but they quickly dissociate within 5 ns MD simulations. Salt and water molecules are not shown for clarity.*

3.2 Free Energy Barriers to Peptide Translocation

We used umbrella sampling to obtain potentials of mean force (PMF) for peptide translocation across the lipid bilayer (see Figure. 3). For both force fields, we obtained the consistent result that ARG8 binds more strongly than LYS8 to the DOPE/DOPS bilayer surface. The CHARMM force field estimates the binding free energies (PMF minimum) of -31.0 kJ/mol for ARG8 and -14.0 kJ/mol for LYS8, while the SLIPID/AMBER combination gives -62.2 kJ/mol for ARG8 and -26.7 kJ/mol for LYS8. The difference between the two force fields is reflected in the predicted peptide structures. The CHARMM force field gives more compact structures for both ARG8 and LYS8 (see Figure S2) and hence fewer energetically favourable contacts occur between the peptide and lipid molecules. The PMF curves also predict extremely high free energy barriers to translocation (~100 k_BT) for both ARG8 and LYS8. The specific free energy barriers to ARG8 translocation through the membrane is ~280 kJ/mol for the CHARMM force field and ~230 kJ/mol for the SLIPID/AMBER model. In this context, it is worth noting that the CHARMM force field predicts that a pore is formed

when either ARG8 or LYS8 is close to the bilayer centre. On the other hand, with the SLIPID/AMBER combination, only ARG8 will create a pore. However, even in the presence of pores, it appears that the free energy barriers remain high. These barriers are dominated by the thermodynamic cost of pore formation in a lipid bilayer[7] and there is no evidence of ARG8 substantially lowering this relative to LYS8. Indeed, the size of the free energy barriers indicates that isolated direct translocation events would give rise to similar (and very small) membrane penetration rates for ARG8 and LYS8. These findings are qualitatively consistent with previous simulation work on oligoarginines.[7, 8, 29]

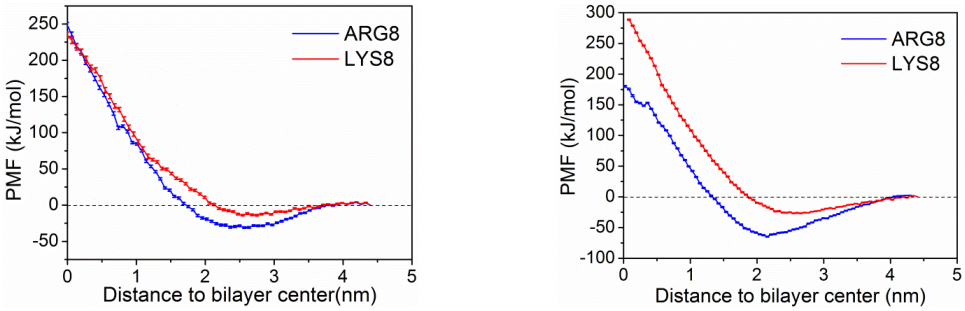

Figure 3. *Free energy profiles for transferring one ARG8 peptide from water to the centre of the DOPE/DOPS lipid bilayer. (A) Results predicted with CHARMM force field; (B) results predicted with SLIPIDS/AMBER99SB-ILDN force field. Each umbrella sampling window was simulated for 100 ns. Error bars indicate statistical precision.*

3.3 ARG8 and LYS8 Effect Significantly Different Kinetics for Pore Closure

Experiments measuring ionic and fluorescent dye transport provide evidence that membrane-active peptides induce membrane pores with a much longer lifetime than transient thermal pores.[30] Coarse-grained simulations by us also found that a variety of membrane-active peptides can significantly stabilize membrane pores.[31] This motivated us to compare the effect of ARG8 and LYS8 peptides on the lifetime of a thermal pore, the creation of which was mimicked by application of a large membrane tension, as described above. If the applied tension were switched off, the

created pore would be expected to close quickly and we found that, without peptide present in the pore, removal of the tension caused the pore to reseal within 30 ns (see Figure. 4A). On the other hand, when one ARG8 was inserted into the pore, it remained open for the duration of the subsequent 800 ns simulation time (Figure. 4B). Surprisingly, in the presence of one LYS8, the pore closed within 10 ns (see Figure. 4C), which was faster than if the peptide were absent. We confirmed these observations in another way. As described in our umbrella sampling simulations above, the CHARMM force field predicted pore formation when both ARG8 and LYS8 are constrained at the membrane centre. Starting with the final configuration from our umbrella simulations, the harmonic tether keeping the peptide in the pore was removed and the system was allowed to relax via unconstrained MD for up to 650 ns. Again, we found that ARG8 kept the pore open over the entire simulation length, while for LYS8 the pore closed within less than 30ns.

Unlike the PMF profiles reported in the previous section, these results reveal substantially different behaviour by ARG8 and LYS8 with respect to their affect on pore closure kinetics, and this is seen in both force field models. Pore closure requires a cooperative reorganization of the lipids lining the pore surface. If several lipids are strongly bound by a peptide, (which appears to be the case with ARG8) pore closure will be slowed. The presence of the peptide causes entropic bottle-necks to what would normally be a rapid resealing process, as lipids must now negotiate the constraints imposed by being strongly bound to a connected sequence of arginine residues. The outcome of this is that the pore dynamics will be tethered to the timescale of surface diffusion of the peptide. On the other hand, the relatively weaker binding of LYS8 is not sufficient to slow lipid diffusion. Indeed, the pore appears to be an overall thermodynamically unfavourable environment for this peptide. This is possibly due to the lower number of water molecules in the pore and the subsequently reduced solvation of the charged residues in LYS8. More rapid closure will then ensue as the peptide diffuses out, simultaneously facilitating the cooperative removal of water molecules from the pore, which have coordinated to the peptide.

Consistent with the discussion above is the expectation that a threshold peptide length is also required to enable kinetic stabilization of pores by ARCPPs. Further simulations using a shorter oligoarginine confirmed this. Figure. 4D shows that if tetraarginine (ARG4) is inserted into the pore instead, it will close relatively quickly (within 50 ns). If kinetic stabilization of pores is crucial to efficient membrane translocation, then this observation is in accord with the measured reduced ability to penetrate membrane pores of oligoarginines with fewer residues.[32] To investigate whether the bilayer charge plays a role in pore stabilization, we inserted peptides into pores created in the purely zwitterionic DOPE and DOPC lipid bilayers. We found that ARG8 maintained the pore over the time of the simulation (250 ns), while for LYS8 the pore closes within tens of nanoseconds (Figure 5). Again, this result is qualitatively similar for both force field models. Hence, while the bilayer charge affects the adsorption of peptide, it is not essential for the significant slowing of pore closure.

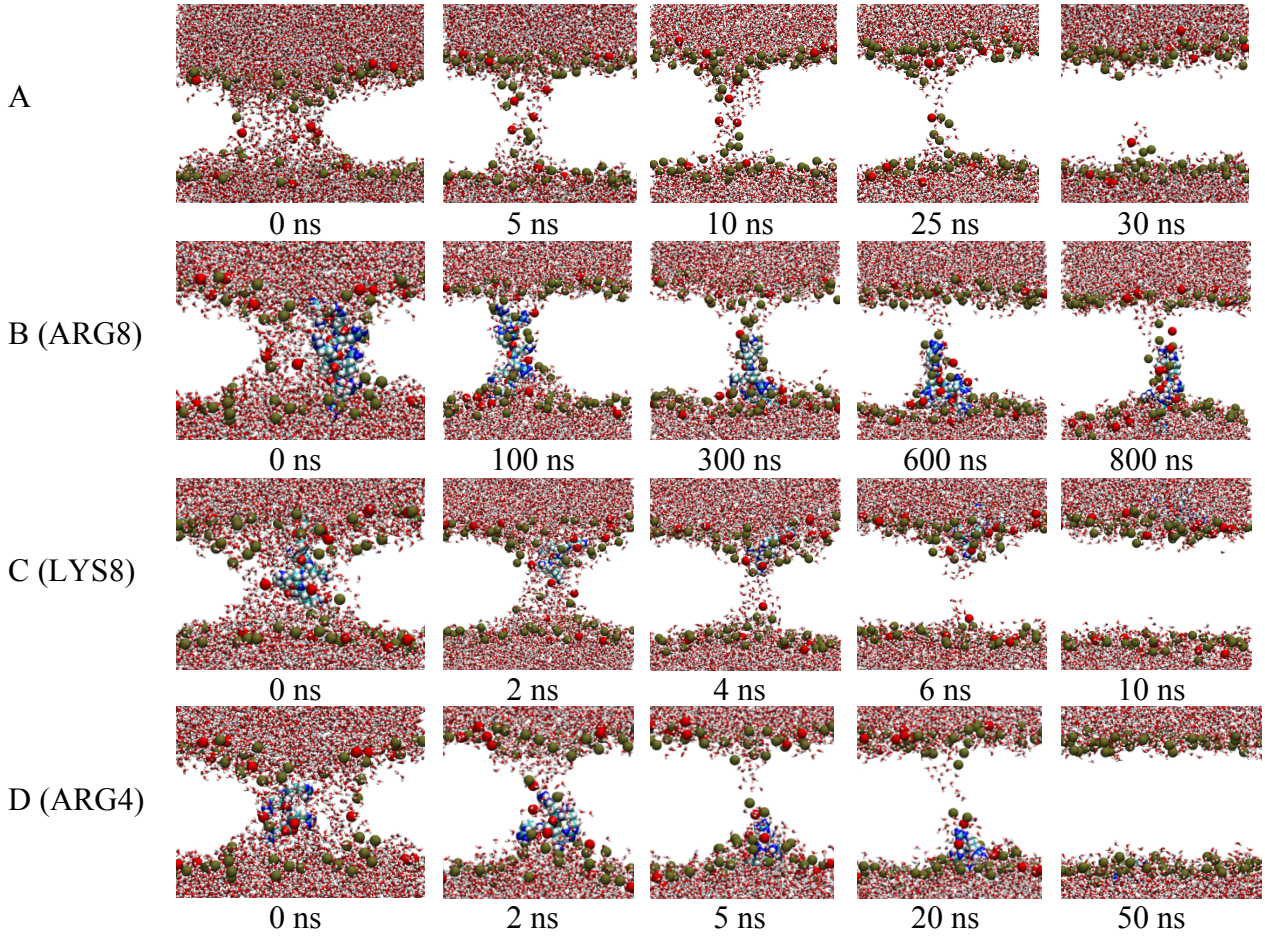

Figure 4. *Snapshot sequences: (A) shows that a tensionless pore in the DOPE/DOPS lipid bilayer quickly reseals within 30 ns. (B) shows that a single ARG8 peptide is able to stabilize a membrane pore in DOPE/DOPS lipid bilayer. (C) shows that a single LYS8 peptide facilitates pore closure. Snapshots (D) show that ARG4 is not able to stabilize the membrane pore. The snapshots were obtained from simulations using the SLIPIDS/AMBER99SB-ILDN force field.*

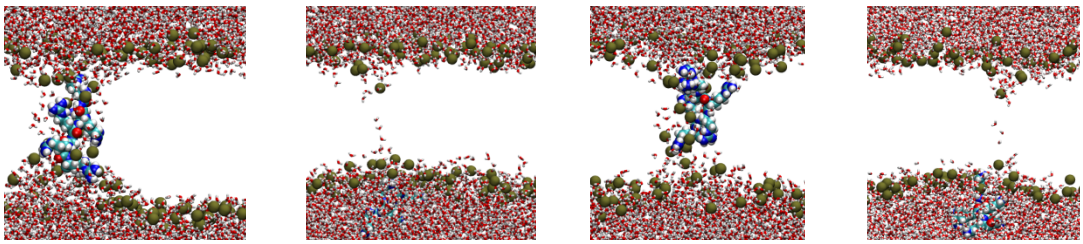

Figure 5. *Snapshot sequence (A) shows that one ARG8 peptide stabilizes the DOPC membrane pore after 250 ns of simulation while snapshot (B) shows that one LYS8 peptide quickly diffuses out of the DOPC membrane pore within 9 ns. Snapshot (C) shows that one ARG8 peptide stabilizes the DOPE membrane pore after 250 ns of simulation and snapshot (D) shows that one LYS8 peptide quickly diffuses out of the DOPE membrane pore within 85 ns.*

In an effort to obtain some physical insights into the modes of action of ARG8 and LYS8, we calculated the average interaction energies of peptides which are constrained to lie within a pore at the centre of the DOPE/DOPS, DOPE and DOPC bilayers. This was achieved by using a harmonic constraint, as employed in the umbrella sampling simulations described earlier. The energies were obtained using the CHARMM force field, as only this force field consistently predicted spontaneous pore formation when either ARG8 or LYS8 is tethered at the bilayer centre (as was observed during umbrella sampling simulations).

By partitioning the average interaction energies into several components in Table 1, we established that ARG8 interacts more strongly than LYS8 with the polar groups of the lipid head and glycerol regions. This is consistent with our PMF calculations, which show that ARG8 has a lower binding free energy with the planar DOPE/DOPS bilayer surface than LYS8, by approximately 17.0 kJ/mol (see Figure 3A). As noted earlier, however, the large differences in the energetic contributions to peptide interactions with the bilayer pore do not appear to significantly affect the relative thermodynamic stability of the pore, with both peptides displaying similar PMF profiles in Figure 3A. The relatively small differences in the PMF of these peptides are likely due to several sources of compensation. For example, if a peptide strongly adsorbs to the bilayer, it will generally relinquish interactions with water. Furthermore, lower thermodynamic energies are usually offset by correspondingly lower entropy contributions to the free energy. Finally, the free energy barrier to peptide translocation may be somewhat insensitive to the degree of peptide interaction with the bilayer, as the peptide remains largely lipid bound (either weakly or strongly) throughout the translocation process. Thus, while the equilibrium thermodynamics of (reversible) translocation is similar for both ARG8 and LYS8, these peptides clearly affect the pore kinetics in significantly different ways, driven by their different lipid interactions.

Table 1. *Electrostatic and Lennard-Jones (LJ) interaction energies of one ARG8 and one LYS8 with water and lipids when the peptide is constrained within pores in DOPE/DOPS, DOPE, and DOPC membranes. The data were obtained by averaging over 50 ns using the CHARMM force field. The energies are expressed in units of kJ/mol.*

Interactions	Peptide-water		Peptide-lipid head		Peptide-glycerol		Peptide-lipid tail	
	ARG8	LYS8	ARG8	LYS8	ARG8	LYS8	ARG8	LYS8
Electrostatics	-963.65	-954.67	-908.01	-901.25	-168.94	-149.96	36.16	16.16
LJ	0.45	4.47	-87.02	-42.69	-78.83	-40.47	-128.73	-80.78

Total(DOPE/DOPS)	-963.20	-950.20	-995.03	-943.94	-247.77	-190.43	-92.57	-64.62
Electrostatics	-1201.17	-1381.73	-1004.73	-515.75	-112.00	-145.34	3.92	1.58
LJ	-65.76	-48.01	-125.41	-75.24	-93.78	-48.35	-83.52	-75.99
Total(DOPC)	-1266.93	-1429.74	-1130.14	-590.99	-205.78	-193.69	-79.60	-74.41
Electrostatics	-952.67	-1079.48	-1220.30	-919.79	-115.37	-240.92	1.95	1.48
LJ	-59.49	-40.93	-105.52	-66.11	-122.61	-66.98	-119.18	-104.11
Total(DOPE)	-1012.16	-1120.41	-1325.82	-985.90	-237.98	-307.90	-117.23	-102.63

During the translocation process, it is possible that more than one peptide may occupy the pore simultaneously. To explore the scenario of multiple pore occupancy, we inserted three peptides into the pore formed in the DOPE/DOPS lipid bilayer. We found that three ARG8 peptides readily aggregated in the pore, despite this peptide adopting segregated configurations on the planar bilayer. The ARG8 aggregate appears to be a disordered complex, which recruits lipids to maintain its stability (Figure. 6A). Furthermore, the aggregate containing pore remains open over the total 900 ns simulation and likely remains kinetically stable while the aggregate is present, due to the expected enormous entropic barriers to pore closure. In contrast, when three LYS8 peptides are placed within the pore, they quickly vacated the region within 70 ns (Figure. 6B). Again, both force field models predict the same qualitative behaviour. Our simulation results suggest that anionic lipids act to screen the electrostatic repulsions between molecules to allow short-ranged attractive interactions between ARG8 molecules to drive aggregation.[33] This screening appears to be more effective in the 3-dimensional environment of the pore, compared with the flat bilayer surface. To test this, we performed bulk phase simulations of peptides and methyl-phosphate counterions. We found ARG8 aggregates in this aqueous environment (Figure. 6C) whereas LYS8 remained dispersed (Figure. 6D).

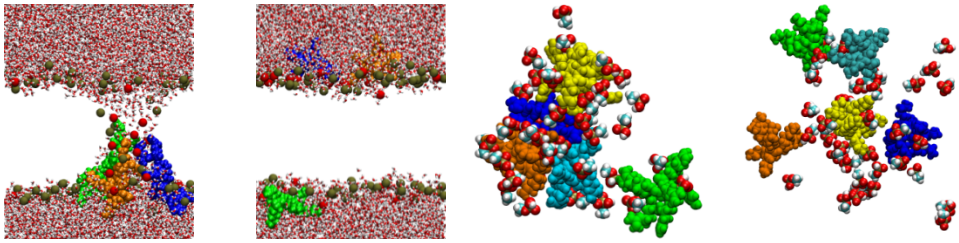

(A) 900 ns (B) 70 ns (C) (D)

Figure 6. *(A) Three ARG8 peptides aggregate in the membrane pore and stabilize the membrane pore by coordinating the lipid head groups. (B) Three LYS8 peptides do not aggregate in the membrane pore. It took approximately 70 ns for the three LYS8 peptides to diffuse out of the pore. (C) In the bulk solution, ARG8 peptides are able to aggregate in the presence of methyl phosphate counterions. (D) In the bulk solution, LYS8 peptides remained separated in the presence of methyl phosphate counterions. In (C-D) water molecules are not shown for clarity.*

3.4 A Cooperative Kinetic Mechanism for ARCPPs Translocation

Taken together, the simulation findings presented above provide new insights into the mechanism by which ARCPPs efficiently pass through lipid membranes, which separate compartments of high (outer) and low (inner) concentration of peptides. The usual arguments for peptide translocation follow a quasi-equilibrium approach, which describes translocation as Brownian dynamics on a (free) energy surface given by PMF profiles, similar to those presented in Figure 3. The translocation rate is then limited by a free energy barrier, which is dominated by the cost of pore formation or, if this is too high, by the free energy cost of lipid defect formation.[34] While adsorbed peptide may facilitate this process to some extent,[35] the free energy penalty for reversible translocation for charged peptides remains very large. Furthermore, as our simulations show, there is apparently little in the PMF profiles that discriminate between ARG8 and LYS8. Thus, it appears that the quasi-equilibrium approach cannot describe the rapid translocation observed for ARCPPs. From our simulations, we are able to suggest a new dynamic model for ARCPP translocation, which is summarized by the following mechanism and illustrated in Figure. 7.

We will describe this mechanism, using the ARG8 peptide as representative of a typical ARCPP. The membrane undergoes thermal fluctuations giving rise to spontaneous pores, which are initially devoid of peptide. While such pores are rare, we expect that normal random processes will cause some of them to become occupied by an ARG8 peptide, drawn from the concentrated outer region. The probability of pore occupation is of course greater, the higher is the peptide concentration in the outer region. Our simulation results suggest that if a thermal pore contains an adsorbed oligoarginine molecule, its kinetics become significantly slowed by that peptide. Thus, once a pore is occupied, it then becomes more likely for other peptides from the outer region to diffuse to it before it is able to close. Indeed, we have found that oligoarginine can aggregate in the pore to produce multiply occupied pores. Continuous translocation can then occur through these "hijacked" pores via cooperative diffusion of peptide molecules via association and dissociation from the aggregate in the pore. Initially, the concentration gradient will favour dissociation of peptide into the inner region. Thus, while the outer peptide concentration remains significantly larger than the inner peptide concentration, the net effect of this process is to cause peptide to effectively translocate through the pore down the peptide concentration gradient. The peptide aggregate plays the role of a "reaction intermediate" which maintains an open pore and hence facilitating efficient peptide translocation. In the meantime, these kinetically stabilized pores are effectively removed from the equilibrium process, which maintains a small but constant concentration of thermally nucleated pores. Thus, we expect the number of kinetically stabilized pores to continue to grow with time.

This mechanism is reminiscent of the so-called Skinner model for ion-permeation through bilayer membranes.[36] The Skinner model has been shown to predict rapid ion transport with only a limited number of pores, stabilized by the formation of pore/ion pairs. Finally, we note that experimental measurements of the trans-activator of transcription (TAT) peptide diffusion on lipid bilayers have indicated the presence of slow and fast diffusing peptide populations, with the slow population being linked to peptide/lipid aggregates within the membrane and ultimately to pore formation.[10]

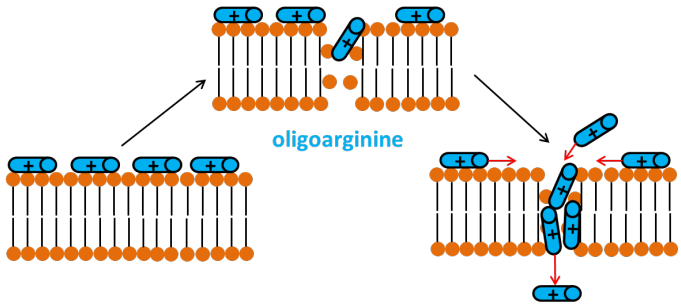

***Figure** 7. A high concentration of cationic arginine-rich peptides exists external to the bilayer with accumulation at the membrane surface. A thermally-activated transient membrane defect (or pore) is formed stochastically in the proximity of one peptide. The peptide associates with the pore via random processes leading to its kinetic stabilization. Peptides subsequently form aggregates in the pore, allowing translocation via diffusion down the peptide concentration gradient through association and dissociation with the aggregate.*

Conclusion

Employing all-atom molecular simulations, we have uncovered remarkable differences in the way that ARG8 and LYS8 interact with lipid bilayers, both on the bilayer surfaces and in the membrane pores. While the equilibrium thermodynamics of peptide translocation is very similar for these peptides, the lifetimes of thermally activated pores is remarkably affected by the type of peptide present within it. This can be explained by the significantly stronger interactions between ARG8 and lipid molecules compared to LYS8. These interactions give rise to entropic bottlenecks in the dynamical processes of pore closure. That is, strong associations between peptide and lipids means that cooperative lipid diffusion (which is likely necessary for pore closure) becomes hindered and the system must wait for rare peptide configurations to occur, before pore closure can occur. We also found that ARG8 peptides are able to aggregate within pores (though not on planar bilayers) aided by electrostatic screening by lipids, as indicated by related bulk phase simulations. These findings have led us to suggest a new cooperative kinetic model to explain the membrane permeation mechanism

of arginine-rich peptides. This mechanism is a departure from the usual quasi-equilibrium approaches, which essentially rely upon a significant lowering of the free energy cost for membrane translocation by ARCPPs. The mechanism by which this can occur remains elusive and is certainly not supported by the PMF calculations presented here. Instead, we propose that the answer to facilitated membrane translocation by ARCPPS may lie with the effect that these peptides have on non-equilibrium kinetics, rather than equilibrium thermodynamics.

AUTHOR INFORMATION

Corresponding Author

* To whom correspondence should be addressed. E-mail: c.woodward@adfa.edu.au.

Author Contributions

The manuscript was written through contributions of all authors. All authors have given approval to the final version of the manuscript.

ACKNOWLEDGMENT

An allocation time from the Lunarc Computing Center at Lund University are gratefully acknowledged. JF acknowledges financial support from the Swedish Research Council.

REFERENCES

(1) Ter-Avetisyan, G.; Tuennemann, G.; Nowak, D.; Nitschke, M.; Herrmann, A.; Drab, M.; Cardoso, M. C. Cell Entry of Arginine-rich Peptides Is Independent of Endocytosis. *J. Biol. Chem.* **2009,** *284*, 3370-3378.

(2) Duchardt, F.; Fotin-Mleczek, M.; Schwarz, H.; Fischer, R.; Brock, R. A Comprehensive Model for the Cellular Uptake of Cationic Cell-Penetrating Peptides. *Traffic* **2007,** *8*, 848-866.

(3) Rothbard, J. B.; Jessop, T. C.; Wender, P. A. Adaptive Translocation: The Role of Hydrogen Bonding and Membrane Potential in the Uptake of Guanidinium-Rich Transporters into Cells. *Adv. Drug Deliv. Rev.* **2005,** *57*, 495-504.

(4) Mishra, A.; Gordon, V. D.; Yang, L. H.; Coridan, R.; Wong, G. C. L. HIV TAT Forms Pores in Membranes by Inducing Saddle-Splay Curvature: Potential Role of Bidentate Hydrogen Bonding. *Angew. Chem. Int. Edit.* **2008,** *47*, 2986-2989.

(5) Sakai, N.; Matile, S. Anion-Mediated Transfer of Polyarginine across Liquid and Bilayer Membranes. *J. Am. Chem. Soc.* **2003,** *125*, 14348-14356.

(6) Mitchell, D. J.; Kim, D. T.; Steinman, L.; Fathman, C. G.; Rothbard, J. B. Polyarginine Enters Cells more Efficiently than Other Polycationic Homopolymers. *J. Pept. Res.* **2000,** *56*, 318-325.

(7) Sun, D. L.; Forsman, J.; Lund, M.; Woodward, C. E. Effect of Arginine-Rch Cell Penetrating Peptides on Membrane Pore Formation and Life-Times: A Molecular Simulation Study. *Phys. Chem. Chem. Phys.* **2014,** *16*, 20785-20795.

(8) Huang, K.; García, A. E. Free Energy of Translocating an Arginine-Rich Cell-Penetrating Peptide across a Lipid Bilayer Suggests Pore Formation. *Biophys. J.* **2013,** *104*, 412-420.

(9) Herce, H. D.; García, A. E.; Litt, J.; Kane, R. S.; Martin, P.; Enrique, N.; Rebolledo, A.; Milesi, V. Arginine-Rich Peptides Destabilize the Plasma Membrane, Consistent with a Pore Formation Translocation Mechanism of Cell-Penetrating Peptides. *Biophys. J.* **2009,** *97*, 1917-1925.

(10) Ciobanasu, C.; Siebrasse, J. P.; Kubitscheck, U. Cell-Penetrating HIV1 TAT Peptides Can Generate Pores in Model Membranes. *Biophys. J.* **2010,** *99*, 153-162.

(11) Antonov, V. F.; Petrov, V. V.; Molnar, A. A.; Predvoditelev, D. A.; Ivanov, A. S. The Appearance of Single-Ion Channels in Unmodified Lipid Bilayer Membranes at the Phase Transition Temperature. *Nature* **1980,** *283*, 585-586.

(12) Meierhenrich, U. J.; Filippi, J. J.; Meinert, C.; Vierling, P.; Dworkin, J. P. On the Origin of Primitive Cells: From Nutrient Intake to Elongation of Encapsulated Nucleotides. *Angew. Chem. Int. Edit.* **2010,** *49*, 3738-3750.

(13) Klauda, J. B.; Venable, R. M.; Freites, J. A.; O'Connor, J. W.; Tobias, D. J.; Mondragon-Ramirez, C.; Vorobyov, I.; MacKerell, A. D.; Pastor, R. W. Update of the CHARMM All-Atom Additive Force Field for Lipids: Validation on Six Lipid Types. *J. Phys. Chem. B* **2010,** *114*, 7830-7843.

(14) Jambeck, J. P. M.; Lyubartsev, A. P. Another Piece of the Membrane Puzzle: Extending Slipids Further. *J. Chem. Theory Comput.* **2013,** *9*, 774-784.

(15) Lindorff-Larsen, K.; Piana, S.; Palmo, K.; Maragakis, P.; Klepeis, J. L.; Dror, R. O.; Shaw, D. E. Improved Side-Chain Torsion Potentials for the Amber ff99SB Protein Force Field. *Proteins: Struct. Funct. Bioinform.* **2010,** *78*, 1950-1958.

(16) Sun, D. L.; Forsman, J.; Woodward, C. E. Evaluating Force Fields for the Computational Prediction of Ionized Arginine and Lysine Side-Chains Partitioning into Lipid Bilayers and Octanol. *J. Chem. Theory Comput.* **2015,** *11*, 1775-1791.

(17) Wimley, W. C.; White, S. H. Experimentally Determined Hydrophobicity Scale for Proteins at Membrane Interfaces. *Nat. Struct. Biol.* **1996,** *3*, 842-848.

(18) Isralewitz, B.; Baudry, J.; Gullingsrud, J.; Kosztin, D.; Schulten, K. Steered Molecular Dynamics Investigations of Protein Function. *J. Mol. Graph. Model.* **2001,** *19*, 13-25.

(19) Torrie, G. M.; Valleau, J. P. Nonphysical Sampling Distributions in Monte Carlo Free-Energy Estimation: Umbrella Sampling. *J. Comput. Phys.* **1977,** *23*, 187-199.

(20) Hub, J. S.; de Groot, B. L.; van der Spoel, D. g_wham-A Free Weighted Histogram Analysis Implementation Including Robust Error and Autocorrelation Estimates. *J. Chem. Theory Comput.* **2010,** *6*, 3713-3720.

(21) Vazdar, M.; Wernersson, E.; Khabiri, M.; Cwiklik, L.; Jurkiewicz, P.; Hof, M.; Mann, E.; Kolusheva, S.; Jelinek, R.; Jungwirth, P. Aggregation of Oligoarginines at Phospholipid Membranes: Molecular Dynamics Simulations, Time-Dependent Fluorescence Shift, and Biomimetic Colorimetric Assays. *J. Phys. Chem. B* **2013,** *117*, 11530-11540.

(22) Hoover, W. G. Canonical dynamics: equilibrium phase-space distributions. *Phys. Rev. A* **1985,** *31*, 1695-1697.

(23) Nosé, S. A. A molecular dynamics method for simulations in the canonical ensemble. *Mol. Phys.* **1984,** *52*, 255-268.

(24) Parrinello, M.; Rahman, A. Polymorphic Transitions in Single Crystals: A New Molecular Dynamics Method. *J. Appl. Phys.* **1981,** *52*, 7182-7190.

(25) Essmann, U.; Perera, L.; Berkowitz, M. L.; Darden, T.; Lee, H.; Pederden, L. G. A Smooth Particle Mesh Ewald Method. *J. Chem. Phys.* **1995,** *103*, 8577-8592.

(26) Hess, B.; Bekker, H.; Berendsen, H. J. C.; Fraaije, J. G. E. M. LINCS: A Linear Constraint Solver for Molecular Simulations. *J. Comput. Chem.* **1995,** *18*, 1463-1472.

(27) Miyamoto, S.; Kollman, P. A. Settle: An Analytical Version of the SHAKE and RATTLE Algorithm for Rigid Water Models. *J. Comput. Chem.* **1992,** *13*, 952-962.

(28) Van der Spoel, D.; Lindahl, E.; Hess, B.; Groenhof, G.; Mark, A. E.; Berendsen, H. J. C. GROMACS: Fast, Flexible, and Free. *J. Comput. Chem.* **2005,** *26*, 1701-1718.

(29) Hu, Y.; Liu, X. R.; Sinha, S. K.; Patel, S. Translocation Thermodynamics of Linear and Cyclic Nonaarginine into Model DPPC Bilayer via Coarse-Grained Molecular Dynamics Simulation: Implications of Pore Formation and Nonadditivity. *J. Phys. Chem. B* **2014,** *118*, 2670-2682.

(30) Almeida, P. F.; Pokorny, A. Mechanisms of Antimicrobial, Cytolytic, and Cell-Penetrating Peptides: From Kinetics to Thermodynamics. *Biochemistry* **2009,** *48*, 8083-8093.

(31) Sun, D. L.; Forsman, J.; Woodward, C. E. Amphipathic Membrane-Active Peptides Recognize and Stabilize Ruptured Membrane Pores: Exploring Cause and Effect with Coarse-Grained Simulations. *Langmuir* **2015,** *31*, 752-761.

(32) Futaki, S.; Suzuki, T.; Ohashi, W.; Yagami, T.; Tanaka, S.; Ueda, K.; Sugiura, Y. Arginine-Rich Peptides - An Abundant Source of Membrane-Permeable Peptides Having Potential as Carriers for Intracellular Protein Delivery. *J. Biol. Chem.* **2001,** *276*, 5836-5840.

(33) Vazdar, M.; Uhlig, F.; Jungwirth, P. Like-Charge Ion Pairing in Water: An Ab Initio Molecular Dynamics Study of Aqueous Guanidinium Cations. *J. Phys. Chem. Lett.* **2012,** *3*, 2021-2024.

(34) Movileanu, L.; Popescu, D.; Ion, S.; Popescu, A. I. Transbilayer Pores Induced by Thickness Fluctuations. *Bull. Math. Biol.* **2006,** *68*, 1231-1255.

(35) Blicher, A.; Wodzinska, K.; Fidorra, M.; Winterhalter, M.; Heimburg, T. The Temperature Dependence of Lipid Membrane Permeability, its Quantized Nature, and the Influence of Anesthetics. *Biophys. J.* **2009,** *96*, 4581-4591.

(36) Bordi, F.; Cametti, C.; Naglieri, A. Ionic Transport in Lipid Bilayer Membranes. *Biophys. J.* **1998,** *74*, 1358-1370.

Table of contents graphic

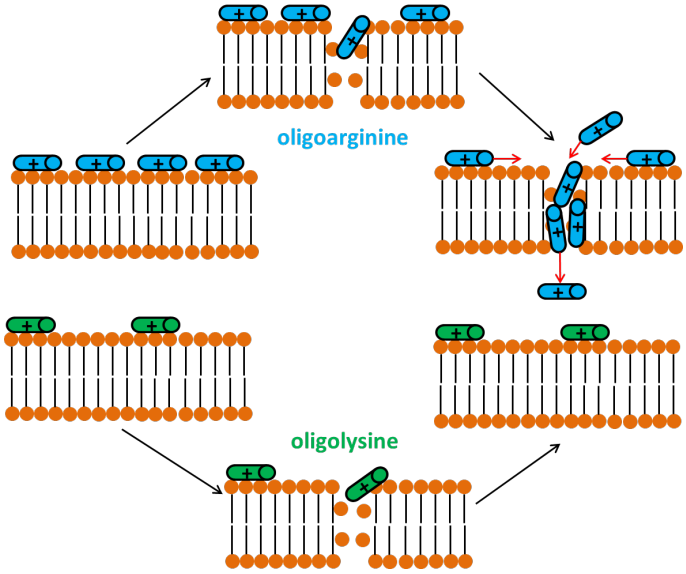

Molecular simulation results suggest a new kinetics controlled model for membrane translocation of arginine-rich peptides.